

Inositol polyphosphates and target of rapamycin kinase signalling govern photosystem II protein phosphorylation and photosynthetic function under light stress in *Chlamydomonas*

Inmaculada Couso¹ , Amanda L. Smythers² , Megan M. Ford² , James G. Umen³ , José L. Crespo¹  and Leslie M. Hicks² 

¹Instituto de Bioquímica Vegetal y Fotosíntesis, Universidad de Sevilla, Avda. Américo Vespucio, 49, Sevilla 41092, Spain; ²Department of Chemistry, University of North Carolina at Chapel Hill, Chapel Hill, NC 27599, USA; ³Donald Danforth Plant Science Center, St Louis, MO 63132, USA

Summary

Authors for correspondence:

Inmaculada Couso
Email: icouso@us.es

Leslie M. Hicks
Email: lmhicks@email.unc.edu

Received: 15 August 2021
Accepted: 9 September 2021

New Phytologist (2021)
doi: 10.1111/nph.17741

Key words: autophagy, *Chlamydomonas reinhardtii*, inositol pyrophosphates, phosphorylation, photosynthesis, target of rapamycin (TOR).

- Stress and nutrient availability influence cell proliferation through complex intracellular signalling networks. In a previous study it was found that pyro-inositol polyphosphates (InsP₇ and InsP₈) produced by VIP1 kinase, and target of rapamycin (TOR) kinase signalling interacted synergistically to control cell growth and lipid metabolism in the green alga *Chlamydomonas reinhardtii*. However, the relationship between InsPs and TOR was not completely elucidated.
- We used an *in vivo* assay for TOR activity together with global proteomic and phosphoproteomic analyses to assess differences between wild-type and *vip1-1* in the presence and absence of rapamycin.
- We found that TOR signalling is more severely affected by the inhibitor rapamycin in a *vip1-1* mutant compared with wild-type, indicating that InsP₇ and InsP₈ produced by VIP1 act independently but also coordinately with TOR. Additionally, among hundreds of differentially phosphorylated peptides detected, an enrichment for photosynthesis-related proteins was observed, particularly photosystem II proteins. The significance of these results was underscored by the finding that *vip1-1* strains show multiple defects in photosynthetic physiology that were exacerbated under high light conditions.
- These results suggest a novel role for inositol pyrophosphates and TOR signalling in coordinating photosystem phosphorylation patterns in *Chlamydomonas* cells in response to light stress and possibly other stresses.

Introduction

Post-translational modifications (PTMs) rapidly regulate major cellular processes such as transcription, translation and metabolism. Understanding these events is essential to map the complex signalling networks mediated by master regulators such as target of rapamycin (TOR) kinase (Soulard *et al.*, 2010; Yu *et al.*, 2011; Robitaille *et al.*, 2013; Roustan & Weckwerth, 2018; Van Leene *et al.*, 2019; Werth *et al.*, 2019; Scarpin *et al.*, 2020). This highly conserved Ser/Thr kinase responds to nutrient availability, energy levels and stress (Loewith & Hall, 2011; Albert & Hall, 2014; González & Hall, 2017), and is connected to growth regulation, cell cycle progression, circadian clock, photosynthesis, autophagy, and nutrient sensing in photosynthetic organisms (Dobrenel *et al.*, 2016; Pérez-Pérez *et al.*, 2017; Schepetilnikov & Ryabova, 2018; Shi *et al.*, 2018; Caldana *et al.*, 2019; Ford *et al.*, 2019; Couso *et al.*, 2020). TOR also participates in the regulation of processes such as carbon assimilation and lipid

accumulation through synergistic coordination with inositol polyphosphates (InsPs) (Couso *et al.*, 2016).

Inositol polyphosphates are phosphorylated derivatives of the myo-inositol ring that can be sequentially and reversibly phosphorylated on all six carbons. InsPs have distinct properties that operate across signalling cascades for the regulation of biological processes throughout the cell, including nutritional sensing and hormone signalling (Tan *et al.*, 2007; Laha *et al.*, 2015; Livermore *et al.*, 2016; Wild *et al.*, 2016; Wu *et al.*, 2016). Among different InsPs, inositol pyrophosphates (PP-InsPs) stand out as secondary messengers due to the presence of 'high energy' pyrophosphate moieties and their ubiquitous nature in eukaryotic cells (Wilson *et al.*, 2013; Shears, 2015). The most common PP-InsPs arise from conversion of InsP₆ to 1-diphosphoinositol 2,3,4,5,6-pentakisphosphate (1-InsP₇ or 1PP-InsP₅), 5-diphosphoinositol 1,2,3,4,6-pentakisphosphate (5-InsP₇ or 5PP-InsP₅) and 1,5-bis-diphosphoinositol 2,3,4,6-tetrakisphosphate (InsP₈ or 1,5(PP)₂-InsP₄) (Supporting Information Fig. S1), in

reactions catalysed by two distinct classes of enzymes: diphosphoinositol pentakisphosphate kinase (PPIP5K, known as VIH in plants and VIP1 in budding yeast and algae) and inositol hexakisphosphate kinase (IP6K, known as KCS1 in budding yeast) (Saiardi *et al.*, 1999; Saiardi, 2004; Mulugu *et al.*, 2007; Laha *et al.*, 2015; Couso *et al.*, 2016; Shears & Wang, 2019). IP6K is not conserved in green organisms; however ITPKs, which are responsible for the conversion of InsP₃ into InsP₅, has recently been suggested to phosphorylate InsP₆ *in vitro* in *Arabidopsis* (Cridland & Gillaspay, 2020). Although, PP-InsPs constitute a minor portion of the InsPs pool, they are suggested to play a fundamental role in controlling metabolism, interacting with SPX domain-containing proteins that are connected to polyphosphate (Poly-P) synthesis (Wild *et al.*, 2016; Gerasimaite *et al.*, 2017) and phosphate signalling in yeast, mammals, and plants (Saiardi, 2012a; Secco *et al.*, 2012; Livermore *et al.*, 2016; Wild *et al.*, 2016; Jung *et al.*, 2018; Zhu *et al.*, 2019; Li *et al.*, 2020; Ried *et al.*, 2021). Furthermore, PP-InsPs have been connected to carbon metabolism in algae (Couso *et al.*, 2016) and jasmonate response in plants (Laha *et al.*, 2015).

In *Chlamydomonas*, a mutation in one of two VIP paralogues (Cre03.g185500), *vip1-1*, was isolated in a screen for increased sensitivity to the TOR-specific inhibitor rapamycin (Rap) (Couso *et al.*, 2016). *vip1-1* was also hypersensitive to other TOR inhibitors, torin1 and AZD8055, indicating a specific interaction between the TOR and InsPs signalling pathways (Couso *et al.*, 2016). Interestingly, *vip1-1* showed misregulation in carbon assimilation and partitioning, displaying irregular levels of tricarboxylic acid (TCA) cycle intermediates and an overaccumulation of storage lipids. This overaccumulation was exacerbated in the presence of Rap and under nitrogen starvation conditions, both of which downregulate TOR, further supporting an interaction between these two signalling pathways (Couso *et al.*, 2016). However, more work is needed to understand this interaction, as PP-InsPs and TOR crosstalk has only been reported in *Arabidopsis* and *Chlamydomonas* (Couso *et al.*, 2016; Van Leene *et al.*, 2019).

In this study, we monitored the phosphorylation levels of RPS6 (a downstream target of TOR signalling) and the autophagy marker ATG8 in *vip1-1* compared with wild-type after Rap treatment. These results indicated a positive downstream synergy of PP-InsPs and TOR kinase on the regulation of these two well known TOR targets. To further explore which processes are either shared or specifically regulated by these signalling pathways, we performed global/phosphoproteomic analysis of *vip1-1* and wild-type before and after Rap treatment. Markedly, the proteomic analysis indicated differential abundance of proteins and decrease in phosphorylation of annotation terms related to photosynthesis between wild-type and *vip1-1*. These results led us to evaluate photosynthetic capacity in *vip1-1* by measuring chlorophyll fluorescence and comparing InsPs levels in *vip1-1* and photosynthetic deficient mutants under low and high light conditions. These data uncovered a novel relationship between TOR and PP-InsPs signalling compounds in governing photosystem II (PSII) and photoprotection that provide new insights in the study of

photosynthetic control in the model green alga *Chlamydomonas reinhardtii*.

Materials and Methods

Cell culturing and rapamycin treatment

Chlamydomonas reinhardtii strain CC-1690 wild-type MT+ (Sager 21gr) (Sager, 1955) was used as parental strain to be compared with *vip1-1*. This strain was isolated in an insertional mutant screen in CC-1690 using the hygromycin resistance gene *aph7* (Couso *et al.*, 2016). All cultures were maintained on TAP (Tris acetate phosphate) agar plates and grown in 350 ml TAP liquid cultures at 25°C. Experiments were performed using five replicate cultures grown to exponential phase ($1-2 \times 10^6$ cells ml⁻¹) for control and Rap treatment, and quenched with cold 40% methanol stored at -80°C before harvesting by centrifuging at 4000 g for 5 min and discarding the supernatant as described in Werth *et al.* (2019). For rapamycin-treated (LC Laboratories, Woburn, MA, USA) cultures, the drug was added to a final concentration of 500 nM from 1 mM stocks in dimethyl sulfoxide (DMSO) for 15 min before harvesting. For control replicates, just drug vehicle (DMSO) without a chemical inhibitor was added to each replicate culture for 15 min before harvesting.

Proteomic analysis

Global protein extraction and phosphopeptide enrichment were performed using frozen pellets as described in Werth *et al.* (2019) (Fig. S2). Phosphopeptide samples were resuspended in 20 µl of 5% acetonitrile, 0.1% TFA while global samples were resuspended to a concentration of 0.2 µg µl⁻¹ in 5% acetonitrile, 0.1% TFA. Global and enriched samples were analysed using an Acquity M-Class UPLC system (Waters, Milford, MA, USA) coupled to a Q-Exactive HF-X Hybrid Quadrupole Orbitrap mass spectrometer (ThermoFisher, Waltham, MA, USA). Raw data were processed using PROGENESIS QI for Proteomics (Non-linear Dynamics; Waters) and parsed using custom R scripts (<https://github.com/hickslab/QuantifyR>) as described previously (Ford *et al.*, 2019). The mass spectrometry proteomics data were deposited to the ProteomeXchange Consortium via the PRIDE partner repository (Vizcaíno *et al.*, 2014, 2016) and can be accessed with the Identifier PXD023085. Detailed methods are available in the Supporting Information (Methods S1) including immunoblot analysis.

Determination of chlorophyll fluorescence

Fluorescence of chlorophyll *a* was measured at room temperature using a pulse-amplitude modulation fluorometer (DUAL-PAM-100; Walz, Effeltrich, Germany) using mid-log phase cultures growing at control (50 µmol m⁻² s⁻¹) and high light (800 µmol m⁻² s⁻¹) conditions. Samples were normalised to 15 µg ml⁻¹ Chl*a* after extraction with 80% acetone (Finazzi *et al.*, 1999). The maximum quantum yield of PSII was assayed

after incubation of the algal suspensions in the dark for 15 min by calculating the ratio of the variable fluorescence, F_v , to maximal fluorescence, F_m (F_v/F_m). The parameters Y(II) and nonphotochemical quenching (NPQ) were calculated using DUAL-PAM-100 software according to the equations in Kramer *et al.* (2004) and Klughammer & Schreiber (2008). Measurements of linear electron transport rates (ETR II) were based on chlorophyll fluorescence of dark-adapted samples applying stepwise increasing actinic light intensities up to $1250 \mu\text{mol m}^{-2} \text{s}^{-1}$. Error bars indicate standard deviation (SD) of the values obtained from experiments performed in triplicate. Imaging-PAM M-series Maxi (Walz) was used to monitor F_v/F_m in *Chlamydomonas* under 50 and $800 \mu\text{mol m}^{-2} \text{s}^{-1}$.

ATP levels

ATP was assessed via LC-MS/MS analysis and 10 mg of fresh weight powder was extracted with trichloroacetic acid (TCA; Thermo Fisher Scientific, Waltham, MA, USA) as described in Weiner *et al.* (1987). Recovery experiments were carried out by adding analyte standards of ATP (Merck KGaA, Darmstadt, Germany) to the frozen tissue before the extraction and the analysis was performed as described in Lunn *et al.* (2006).

InsPs extraction and analysis

For InsP₇ and InsP₈ extraction, 300 ml of mid-log phase culture per sample was collected at a cell density of 2×10^6 cells ml⁻¹. Samples were extracted as reported in Couso *et al.* (2016) and 1 μM 3-fluoro-InsP₃ (Enzo Life Sciences, Farmingdale, NY, USA) was used as internal standard for normalisation for relative quantification of the same InsPs species.

LC-MS/MS data were acquired using a Q-Exactive mass spectrometer (Thermo Fisher Scientific) equipped with a 1200

Capillary LC system (Agilent, Santa Clara, CA, USA) and a $0.5 \times 150\text{-mm}$ 5- μm BioBasic AX Column (Thermo Fisher Scientific) using the conditions reported in Couso *et al.* (2016). Mean data and SD were calculated from three biological replicates, each of which had three technical replicates.

Results

TOR activity is misregulated in *vip1-1* after rapamycin inhibition

The insertional mutant *vip1-1* is PP-InsPs deficient and displays hypersensitivity to TOR inhibition by Rap (Couso *et al.*, 2016). To further investigate the regulation of TOR in the *vip1-1* mutant, RPS6 phosphorylation was monitored over time in WT and *vip1-1* cells treated with Rap. We previously demonstrated that phosphorylation of RPS6 on Ser245 is a readout of TOR activity in *Chlamydomonas* (Couso *et al.*, 2020). The basal phosphorylation level of RPS6 Ser245 (P-RPS6) was similar in both strains. However, *vip1-1* showed a significant decrease in P-RPS6 compared with WT (Fig. 1a,b) after 30 min of Rap treatment that was more pronounced after 60 min (Fig. 1b,c) indicating a faster de-phosphorylation in *vip1-1* compared with WT. The P-RPS6/RPS6 levels were similar in WT and *vip1-1* cells only after 90 min.

The detection of lipidated ATG8 (ATG8-PE) is an effective method to monitor autophagy; ATG8-PE accumulates under autophagy-inducing conditions including TOR inhibition (Pérez-Pérez *et al.*, 2010). The levels of ATG8 and ATG8-PE were similar in WT and *vip1-1* cells under control conditions (Fig. 1d). However, both ATG8 and ATG8-PE were more highly accumulated in *vip1-1* after 30 min Rap treatment compared with WT (Fig. 1d), indicating a faster and stronger activation of autophagy in *vip1-1*. RPS6 was previously demonstrated to be

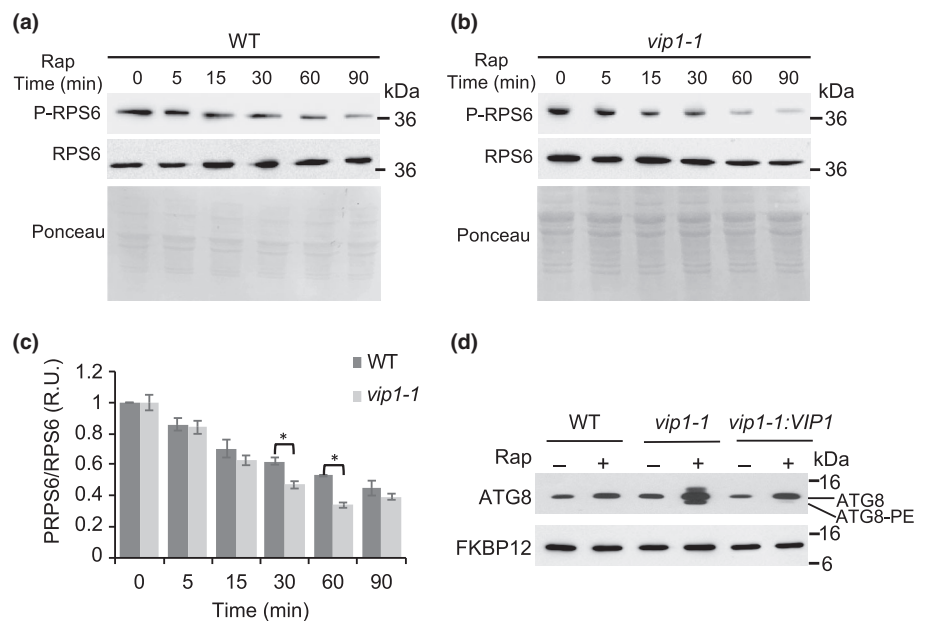


Fig. 1 Immunoblot analysis of P-RPS6/RPS6 as a readout of target of rapamycin kinase activity in *Chlamydomonas* WT (a) and *vip1-1* (b) in the presence of rapamycin (Rap) along a time course. Relative quantitation of P-RPS6/RPS6 was made using three biological replicates. Error bars represent standard deviation of the mean values. Asterisks represent significant differences ($P < 0.05$) evaluated using Student's *t*-test. (c). Immunoblot analysis of ATG8 in the presence or absence of rapamycin for 30 min. FKBP12 was used as loading control (d).

rapidly turned over by autophagy in *Chlamydomonas* (Couso *et al.*, 2018), therefore explaining the reduced abundance of this protein in *vip1-1* after 60 min (Fig. 1b).

Gene ontology analysis in *vip1-1* proteomics reveals an especial enrichment for PSII

Quantitative proteomics were performed in WT and *vip1-1* cells under control conditions and following 15 min of Rap treatment as previously reported in Werth *et al.* (2019), through which 2460 proteins were quantified (Table S1). No proteins significantly changed in abundance between control and Rap-treated conditions (Fig. S3A), confirming minimal protein turnover after 15 min Rap treatment. However, we observed significant differences in basal levels of proteins between the noninhibited samples for each strain (Fig. S3B). Despite having similar growth rates as the WT strain (Couso *et al.*, 2016), 545 proteins from *vip1-1* were differentially abundant compared with the parent strain, with 373 increased and 172 decreased (Table S1).

Quantitative phosphoproteomic analysis of *vip1-1* and WT cells identified 3986 unique phosphorylated phosphopeptides, referred to as identifiers, derived from 1935 proteins (Table S2). Given the lack of significant changes in protein abundance within a given strain in the global proteomic analysis following Rap treatment (Fig. S3A; Table S1), changes in phosphopeptide abundance is likely to correspond to changes in phosphorylation state rather than changes in total protein abundance, enabling robust analysis of phosphorylation signalling pathways. Following Rap treatment, 1029 identifiers significantly changed in *vip1-1*, with 228 decreasing and 801 increasing (Fig. 2a), while 217 identifiers significantly changed in the parent strain, with 129 decreasing and 88 increasing (Fig. 2b). Comparison of the two strains yielded 1625 identifiers differentially abundant before Rap treatment (Fig. 2c) and 346 identifiers following treatment (Fig. 2d).

Gene ontology (GO) enrichment analysis (Ashburner *et al.*, 2000) of the global proteomic dataset of untreated cultures

revealed that *vip1-1* was enriched over WT in biological functions related to stress responses, including protein folding, photosystem II (PSII) repair, cellular response to oxidative stress, and protein refolding (Fig. S4A). By contrast, *vip1-1* was deficient in GO terms related to cellular metabolism, including the tricarboxylic acid cycle and electron transport in PSII, among others (Fig. S4B).

Gene ontology analysis of significantly changed phosphopeptides in *vip1-1* following Rap treatment uncovered an enrichment of identifiers involved in RNA processing as well as chromatin and DNA binding (Fig. 3a). By contrast, identifiers significantly decreasing in *vip1-1* under the same treatment were enriched in photosynthesis-related GO terms, including PSII assembly, PSII stabilisation, and the PSII oxygen evolving complex (Fig. 3b), indicating an important role of PP-InsPs in the regulation of photosynthetic-related processes in *Chlamydomonas* that has not been reported in green organisms therefore far. Notably, enrichment of photosynthesis-related proteins was not detected in WT (Fig. S5).

Differential phosphorylation of known and putative TOR substrates are found in *vip1-1*

In total, 48 phosphorylated identifiers from 22 proteins with homology to known TOR signalling-related proteins were identified in this study (Table S3). Under Rap treatment, 11 of these identifiers significantly increased and two significantly decreased in *vip1-1* while one identifier significantly increased and four significantly decreased in the parent strain, with no overlap between strains (Table S3). One of these identifiers was an uncharacterised phosphosite, S2598 on TOR (Cre90.g400553.t1.1), that was significantly increased in the *vip1-1* mutant following Rap treatment (\log_2FC : 2.31) but did not change in the parent strain (Table S3).

An identifier from the autophagy-related protein ATG11 (Cre16.g651350.t1.1-S1176) was also found to significantly decrease in *vip1-1* (\log_2FC : -1.44) (Table S3) compared with WT under control conditions. ATG11 is indispensable for the initiation of autophagy in different eukaryotes (Sun *et al.*, 2013; Li *et al.*, 2014).

The La-domain RNA-binding (LARP1) protein is an effector of mTORC1 that regulates TOP mRNAs and is connected to cell cycle progression and embryogenesis in mammals (Fonseca *et al.*, 2015; Philippe *et al.*, 2020). In this study, six significantly changing identifiers were detected in *Chlamydomonas* LARP1 (Cre10.g441200.t1.2), three significantly decreased in *vip1-1* compared with WT in control conditions (S529, T668, S670), two increased in the *vip1-1* mutant under Rap treatment (S670, S812), and only one changed after Rap treatment in WT (S817) (Table S3).

Phosphorylation of PSII core components are downstream PP-InsPs and TOR signalling

In this study, global protein analysis uncovered 155 proteins related to photosynthesis, photorepair, and chlorophyll biosynthesis

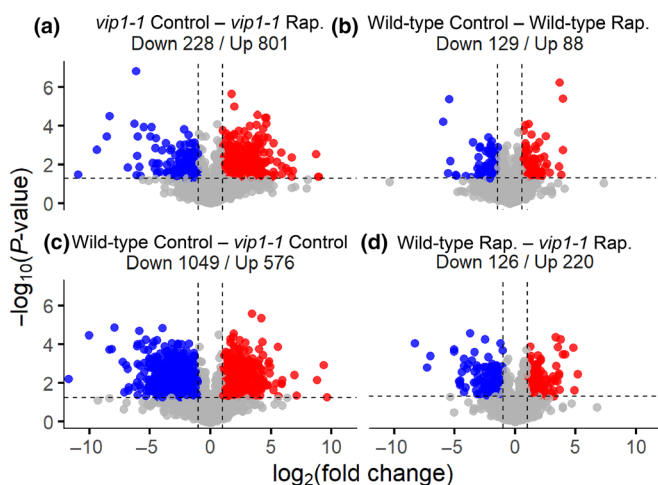


Fig. 2 Phosphoproteomic data represented in volcano plots of two-tailed equal variance *t*-tests between each *Chlamydomonas* strain with or without rapamycin (Rap) treatment (a, c) and between strains (b, d).

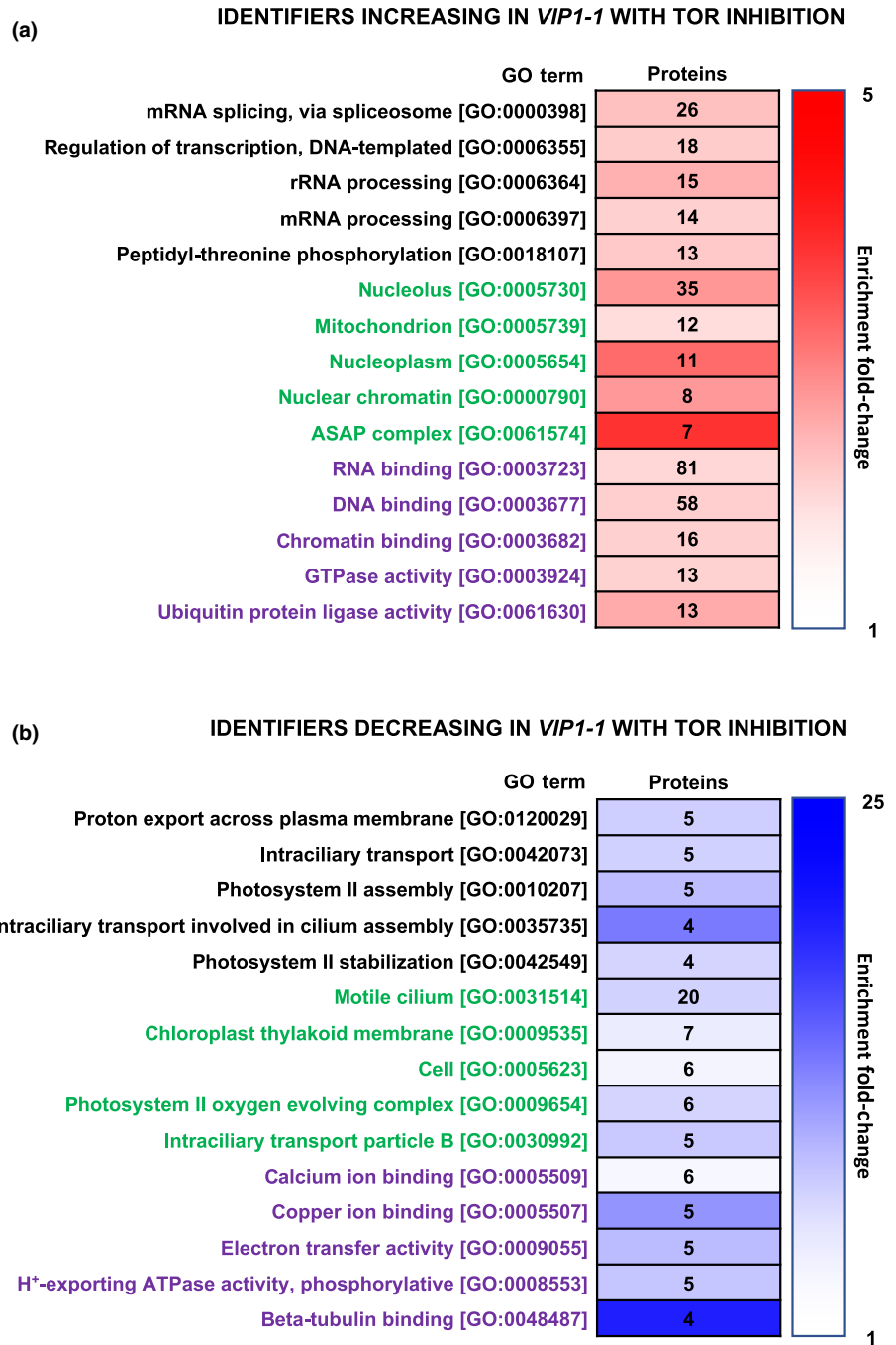


Fig. 3 *Chlamydomonas vip1-1* mutant phosphoproteomic gene ontology (GO) analysis. (a) Count of the number of proteins in the top five biological process (black), cellular component (green) and molecular function (purple) GO terms with a fold-change enrichment of at least 1.5 from identifiers significantly more abundant in *vip1-1* with rapamycin treatment. Cells are shaded to reflect fold-change for each GO term. (b) Count of the number of proteins in the top five biological process (black), cellular component (green) and molecular function (purple) GO terms with a fold-change enrichment of at least 1.5 from identifiers significantly less abundant in *vip1-1* with rapamycin treatment. Cells are shaded to reflect fold-change for each GO term.

(Fig. S4). Among them, 50 proteins displayed differential abundance in the *vip1-1* strain compared with the parent strain, with 34 increased and 16 decreased under control conditions (Table S4). These data suggest less abundant PSII with a significant decrease in four out of the six catalytic subunits, including D1 (gi|41179021|ref|NP_958377.1) and D2 (gi|41179063|ref|NP_958420.1), with \log_2FC of -2.07 and -2.13 , respectively, and the two reaction centre proteins, psbC (CP43; gi|41179065|ref|NP_958422.1) and psbB (CP47; gi|41179032|ref|NP_958388.1), with \log_2FC s of -1.89 and -2.17 , respectively (Table S4).

Phosphopeptide analysis of the photosynthesis-related proteins revealed 72 identifiers from 31 proteins, with 27 identifiers

upregulated and 16 downregulated in *vip1-1* compared with WT (Table S5). Additionally, 15 identifiers were differentially phosphorylated in *vip1-1* compared with WT following TOR inhibition (5 upregulated and 10 downregulated) (Table S5). Phosphorylation of psbC-S456 ($\log_2FC -3.46$) and psbB-T501 ($\log_2FC -4.98$) were highly downregulated in *vip1-1* compared with WT (Fig. 4a; Table S5). Following Rap treatment, the phosphorylation of these identifiers increased in *vip1-1* but no significant differences were detected between WT and *vip1-1* (Table S5). STL1 (Cre12.g483650.t1.2), the *Chlamydomonas* paralogue of STN8 kinase, had significantly less phosphorylation on T126 in *vip1-1* compared with WT before Rap treatment

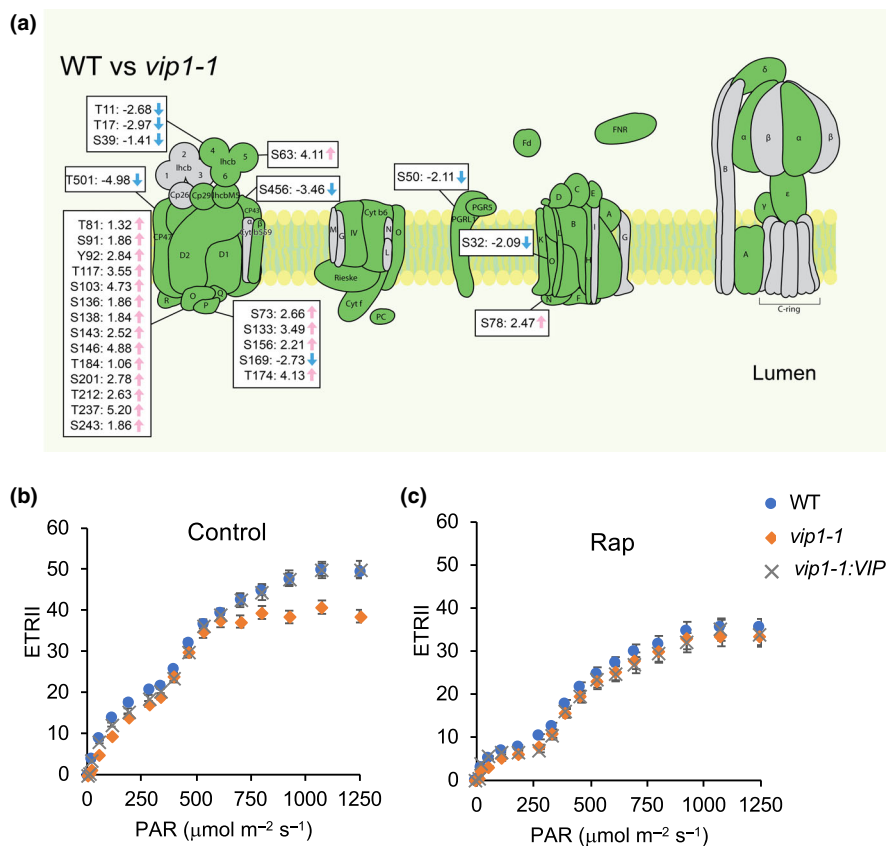


Fig. 4 (a) Differential phosphorylation of the photosynthetic apparatus in the *vip1-1* mutant compared with the *Chlamydomonas* parent strain. Proteins coloured green show proteomic coverage in the dataset while proteins coloured grey do not. Each significantly changing phosphosite was localised on a unique phosphopeptide. Nontransformed fold changes are reported. Pink arrows represent significant upregulated phosphorylation of the indicated identifiers while blue arrows represent significant downregulated phosphorylation of the indicated identifiers (b) Electron transfer rate of PSII (ETRII) measured in a light induction curve using photosynthetically active radiation (PAR) from 0 to 1250 $\mu\text{mol m}^{-2} \text{s}^{-1}$ under control conditions and rapamycin treatment (c) in WT, *vip1-1* and the complemented line (*vip1-1:VIP1*). Errors bars indicate standard deviation of the mean values from three biological and three technical replicates.

(log₂FC -2.06), and this downregulation was compensated after Rap where it was upregulated by a log₂FC of 1.81 (Table S5). This kinase plays a central role in the phosphorylation of the PSII core proteins (Rochaix *et al.*, 2012).

We performed PAM fluorometry under a light induction curve to further investigate PSII defects in *vip1-1*. F_v/F_m was decreased in both the *vip1-1* and WT cells treated with Rap (Table 1) similar to the results reported using the TOR inhibitor AZD 8055 (Ford *et al.*, 2019; Upadhyaya & Rao, 2019). However, we observed that the electron transfer rate of PSII (ETRII) in *vip1-1* was significantly decreased compared with WT after 600 $\mu\text{mol m}^{-2} \text{s}^{-1}$, with the ETRII of *vip1-1* comprising only 12–19% of the rate of the WT (Fig. 4b). Furthermore, at high fluences Rap treatment decreased ETRII of WT that shows similar levels than *vip1-1* cells, which did not change after Rap addition (Fig. 4c). This result suggests that PP-InsPs are involved in the maintenance of electron transfer during high light stress and work constructively with TOR to provide positive regulation of the photosynthetic apparatus under noninhibited conditions, as Rap treatment results in the same decreased ETRII in WT as it is observed in control conditions of *vip1-1*. In addition, the abundance of several photosynthetic repair-specific proteins were upregulated in *vip1-1*, including vesicle-inducing protein in plastids 1 (VIPP1, Cre13.g583550.t1.2; log₂FC 1.62) (Table S4), a multifunctional protein involved in the maintenance of photosystems (Nordhues *et al.*, 2012; Theis & Schroda, 2016; Gupta *et al.*, 2021), and chloroplast DNAJ-like protein 2 (CDJ2,

Table 1 F_v/F_m in *Chlamydomonas reinhardtii* WT, *vip1-1* and complemented line under different conditions.

F_v/F_m	Control	Rap	High light (800 $\mu\text{mol m}^{-2} \text{s}^{-1}$)
WT	0.71 ± 0.003	0.60 ± 0.003	0.63 ± 0.005
<i>vip1-1</i>	0.65 ± 0.002	0.58 ± 0.002	0.08 ± 0.004
<i>vip1-1:VIP1</i>	0.68 ± 0.001	0.61 ± 0.002	0.52 ± 0.003

Values are mean ± SD; $n = 6$.

Cre07.g316050.t1.2; log₂FC 3.54) (Table S4), which interacts with VIPP1 to regulate thylakoid biogenesis (Liu *et al.*, 2005).

Oxygen evolving complex proteins PsbO and PsbP were also differentially phosphorylated (Fig. 4a; Table S5). We found 15 identifiers of PsbO (Cre09.g396213.t1.1) (Table S5), 14 of them upregulated in *vip1-1* before Rap exposure. Two sites, S103 and T237, were highly upregulated in control conditions (log₂FC 4.73 and 5.20, respectively) and highly downregulated (log₂FC -2.93 and -2.33) after Rap treatment. A conserved T212 was also upregulated in the mutant (log₂FC 2.63). Additionally, four identifiers of PsbP (Cre12.g550850.t1.2-S73; -S133; -S156; -S174) (Table S5) were highly upregulated in *vip1-1* (log₂FC 2.66; 3.49; 2.21 and 4.13, respectively) while S169 was downregulated (log₂FC -2.68) in the mutant. S73 and S174 were downregulated in *vip1-1* after Rap treatment (log₂FC -1.71 and -1.70, respectively).

PP-InsPs control abundance and phosphorylation of light harvesting complex II proteins in coordination with TOR

State transitions involve the reversible transfer of a fraction of the light harvesting complex II (LHCII) from photosystem PSII to PSI as a result of protein phosphorylation (Goldschmidt-Clermont & Bassi, 2015). This process balances the excitonic flux of the two PSs to meet the cellular demand for ATP following changes in environmental conditions and protects from overexcitation (Cardol *et al.*, 2009). Under stress conditions, the transition from state 1 to state 2 induces the switch from linear to cyclic electron flow (CEF). Our proteomic analysis indicated that LHCBM5 (Cre03.g156900.t1.2) abundance is decreased in *vip1-1* compared with WT (Table S4). This protein is a component of the light harvesting antenna that migrates from PSII to PSI under state transitions (Takahashi *et al.*, 2006). The downregulation of LHCBM5 was confirmed by immunoblotting, with an observed protein reduction of *c.* 20% (Fig. 5a,b) in *vip1-1* compared with the WT and the complemented line.

LHCb4 (CP29) is a heavily phosphorylated protein in the thylakoid membrane of *Chlamydomonas* (Lemeille *et al.*, 2010; Bergner *et al.*, 2015), with six different identifiers found in this study (Table S5). Among them T11, T17 and S39 were significantly decreased in the mutant under control conditions (\log_2FC -2.68 , -2.97 and -1.41 , respectively) and T11 remained downregulated after Rap treatment. Four identifiers belonging to

LHCb5 (Cre16.g673650.t1.1-T10, -S63, -T187, -S202) were also identified (Table S5), although only S63 was upregulated in *vip1-1* compared with WT (\log_2FC 4.11). This upregulation was prevented in the presence of Rap, further indicating the interaction of PP-InsPs and TOR in controlling the phosphorylation state of LHCb5.

CEF and ATP levels are aberrantly regulated in *vip1-1*

In *Chlamydomonas*, PGRL1 (Cre07.g340200.t1.2) forms a supercomplex with PSI and cytochrome b6/f to initiate CEF (Iwai *et al.*, 2010). In our study, a nonconserved identifier in PGRL1 (Cre07.g340200.t1.2; S50) was downregulated in *vip1-1* (\log_2FC : -2.11) under control conditions and in WT after Rap treatment (\log_2FC : -2.01) (Fig. 4a; Table S5). In *vip1-1*, this downregulation is alleviated after Rap and showed no significant difference compared with WT. These data suggest a compensation mechanism for PGRL1 phosphorylation that is regulated by PP-InsPs and TOR.

Cyclic electron flow is activated after high light stress and rewires energy to increase ATP yield. We identified significant increases in two ATP synthase subunits of *vip1-1* (Table S1): subunit E (gi|4117902|ref|NP_958379.1; \log_2FC 1.67), which forms the connection between the lumal and stromal hemispheres, and subunit II (Cre11.g481450.t1.2; \log_2FC 1.37), which regulates ATP synthesis based on the proton gradient

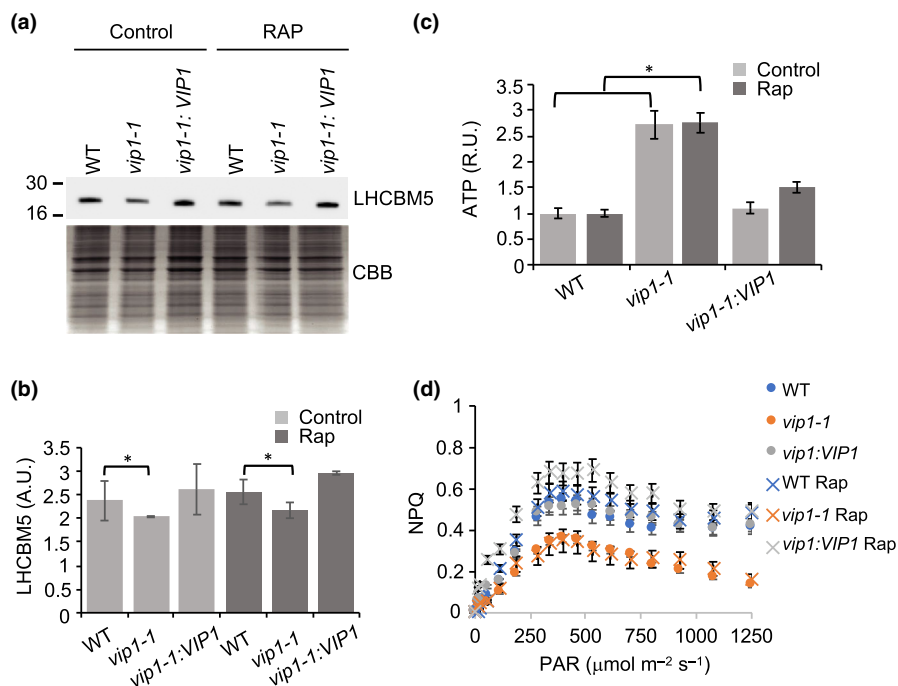


Fig. 5 (a) Immunoblot analysis of LHCBM5 under control conditions and rapamycin treatment (30 min) in *Chlamydomonas* wild-type (WT), *vip1-1* and the complemented line (*vip1-1:VIP1*). (b) Quantitation of LHCBM5 was made using three biological replicates. Error bars represent standard deviation (SD) of the mean values. Asterisks represent significant differences ($P < 0.05$) evaluated using Student's *t*-test. (c) Quantitation of ATP in WT and *vip1-1* mutant under control and rapamycin conditions. Errors bars represent SD of the mean values from three biological replicates. Asterisks represent significant differences ($P < 0.05$) evaluated using Student's *t*-test. (d) Nonphotochemical quenching (NPQ) was measured in WT, *vip1-1* and the complemented line (*vip1-1:VIP1*) on an induction curve using photosynthetically active radiation (PAR) from 0 to 1250 $\mu\text{mol m}^{-2} \text{s}^{-1}$ in the presence or absence of 500 nM rapamycin (Rap). Errors bars indicate SD of the mean values from three biological and three technical replicates.

across the thylakoid membrane (Lemaire & Wollman, 1989; Richter *et al.*, 2000; Hahn *et al.*, 2018). To investigate the effect of the higher abundance of these ATP synthase subunits in the *vip1-1* mutant, we determined the level of ATP in WT, *vip1-1* and complemented cells. Our results indicated that ATP was highly increased in the *vip1-1* mutant (Fig. 5c). While the activation of CEF seems to be dependent on the coordination of PP-InsPs and TOR controlling PGRL1 phosphorylation, PP-InsPs must also be independently controlling the levels of ATP as no significant changes were seen following Rap treatment (Table S1).

Nonphotochemical quenching and PP-InsPs biosynthesis are likely to be connected by a feedback loop

In *Chlamydomonas*, LHCSR3 (Cre08.g367400.t1.1) mediates the induction of NPQ (Peers *et al.*, 2009) and can work together or independently with PGRL1 during high light (HL) acclimation (Chaux *et al.*, 2017). By contrast with the observed downregulation of CrPGRL1-S50, three identifiers of LHCSR3 (Cre08.g367400.t1.1; -S165, -T161, -Y170) (Table S5) were upregulated in *vip1-1* (\log_2FC 1.48, 1.70 and 2.67, respectively). The phosphorylation of two of these phosphosites was decreased following Rap exposure, while Y170 remained upregulated in the mutant under the same conditions (Table S5). To investigate this further, we compared NPQ in WT, *vip1-1* and a complemented line using light response curves and PAM fluorometry in the presence or absence of Rap (Fig. 5d). NPQ was highly downregulated in the *vip1-1* mutant curve compared with the other two strains, reaching a difference of 72% under very HL ($1250 \mu\text{mol m}^{-2}\text{s}^{-1}$) (Fig. 5d). Although, WT and the complemented line keep NPQ levels above 0.4 after reaching HL ($750 \mu\text{mol m}^{-2}\text{s}^{-1}$), *vip1-1* further downregulates NPQ reaching 0.16, indicating that NPQ is not supported by *vip1-1* photosynthetic machinery under HL. In the presence of Rap, NPQ did not change significantly in any of the strains compared with control conditions.

Additionally, F_v/F_m and Y(II) were analysed in WT and *vip1-1* cells under control light ($50 \mu\text{mol m}^{-2}\text{s}^{-1}$), HL ($800 \mu\text{mol m}^{-2}\text{s}^{-1}$) and Rap (control light conditions) conditions (Fig. S6; Table 1). Despite few differences in F_v/F_m under control conditions, *vip1-1* showed significantly reduced F_v/F_m and Y(II) values when subjected to HL, further indicating a misregulation of the light stress compensation mechanisms (Fig. S6A,B; Table 1).

Similarly to downregulated NPQ mutants (*npq1* and *npq2*), *vip1-1* showed decreased NPQ under HL stress (Niyogi *et al.*, 1997, 1998; Kress & Jahns, 2017) (Fig. 6a). To evaluate the link between NPQ, PP-InsPs and TOR, InsP₇ and InsP₈ abundances were determined in WT, *vip1-1* and *npq2* under control and HL conditions. In WT cells, InsP₇ and InsP₈ levels increased significantly after HL treatment (Fig. 6b,c). In fact, InsP₈ levels reached a 50% increase under HL (Fig. 6c). As previously reported (Couso *et al.*, 2016), InsP₇ and InsP₈ were diminished in *vip1-1* compared with WT, which was constant under HL (Fig. 6b,c). For *npq2*, InsP₇ decreased compared with WT in control

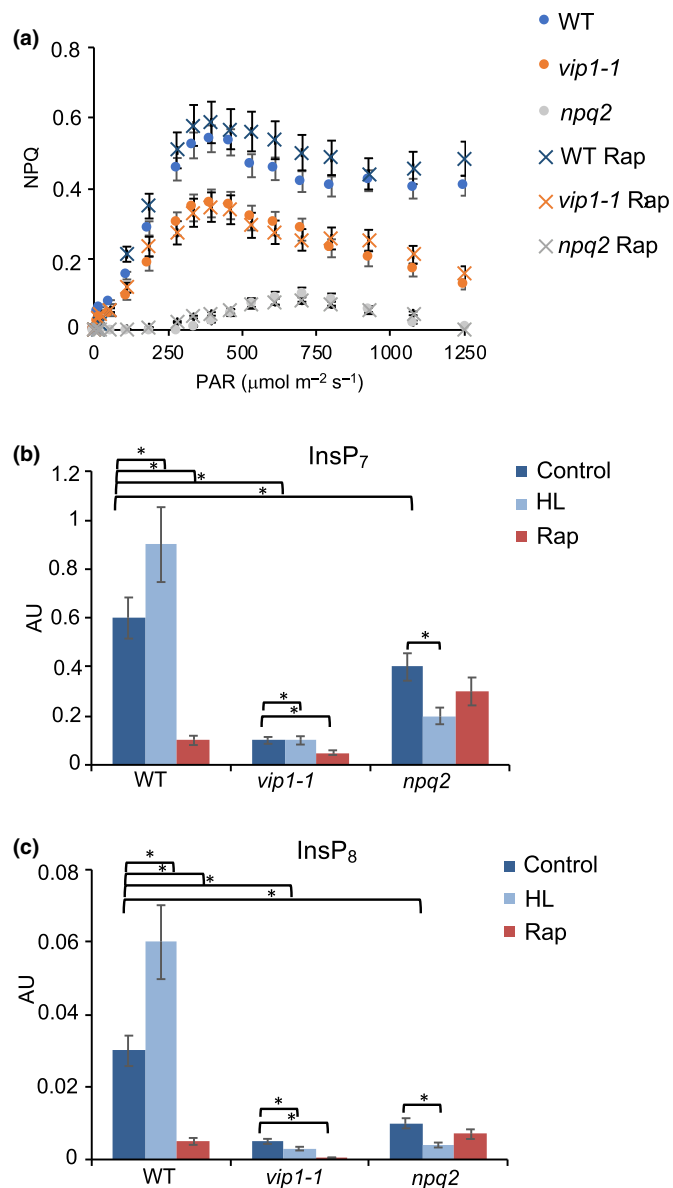


Fig. 6 Nonphotochemical quenching (NPQ) monitoring and pyro-inositol polyphosphates analysis in *Chlamydomonas* WT, *vip1-1* and the *npq2* mutants. (a) NPQ was measured on a light induction curve using photosynthetically active radiation (PAR) from 0 to $1250 \mu\text{mol m}^{-2}\text{s}^{-1}$ in the presence or absence of 500 nM rapamycin (Rap). Errors bars indicate standard deviation (SD) of the mean values from three biological and three technical replicates. Inositol polyphosphate-7 (InsP₇) (b) and inositol polyphosphate-8 (InsP₈) (c) were analysed by liquid chromatography–mass spectrometry (LC-MS) in the three strains under control ($50 \mu\text{mol m}^{-2}\text{s}^{-1}$), high light (HL) ($800 \mu\text{mol m}^{-2}\text{s}^{-1}$) and in the presence of 500 nM Rap at light control conditions. Bar graphs scaled in arbitrary units (AU) and normalised with a standard, 3-fluoro-InsP₃, showing relative levels of inositol polyphosphates (InsPs) species extracted from indicated strains and measured using mass spectrometry. This allows relative quantification of the same InsPs species. Error bars indicate SD from at least three biological replicates. Asterisks represent significant differences ($P < 0.05$) evaluated using Student's *t*-test.

conditions and further decreased under HL treatment (Fig. 6b). InsP₈ was also highly downregulated in *npq2* under HL, reaching 75% and 60% decrease, respectively (Fig. 6c). NPQ and InsP_{7/8}

InsP₈ were also monitored following Rap treatment (30 min) in all strains. There were no significant differences in NPQ after Rap treatment in any of these strains compared with control conditions (Fig. 6a). After Rap treatment, InsP₇ an InsP₈ levels in *npq2* were comparable to the level detected under control light conditions (Fig. 6b,c). These data indicate a novel connection between PP-InsPs levels and NPQ that may control HL stress compensation in *Chlamydomonas* that acted independently of TOR.

Discussion

Pyro-inositol polyphosphates modulate TOR activity in *Chlamydomonas*

The macrolide rapamycin partially arrests cell growth in *Chlamydomonas* (Crespo *et al.*, 2005; Couso *et al.*, 2016), suggesting that it does not completely inhibit TOR activity. This is conserved in mammals (Thoreen *et al.*, 2009), in which differential sensitivity of mTORC1 phosphorylation sites to Rap has been reported as well (Kang *et al.*, 2013). We isolated *vip1-1* in a genetic screen due to its hypersensitivity to Rap compared with WT and have demonstrated a genetic link between pathways by restoring this phenotype in the *vip1fcbp12* double mutant (Couso *et al.*, 2016). In this study, we found that *vip1-1* accelerates TOR inactivation under Rap conditions (Fig. 1a–c), indicating that these signalling pathways are likely to be controlling similar downstream targets either coordinately and/or independently of each other.

InsP₇ is a phosphate donor for different nucleolar proteins in yeast (NSR1 and SRP40) and mammals (Nopp140 and TCOF1) (Saiardi, 2004, 2012b, 2016; Bhandari *et al.*, 2007). The InsP₇-derived phosphate is thought to be attached to a pre-existing phosphorylation (β -pyrophosphorylation), which may provide a unique mode of signalling to proteins. However, the impact of PP-InsPs on phosphorus-signalling networks in photosynthetic organisms has not yet been reported. We used differential analysis of global proteomics and phosphoproteomics in WT and *vip1-1* in the presence or absence of Rap to reveal both the overlap with the TOR signalling network as well as the mechanistic connection between PP-InsPs and PTMs that has not been reported in green organisms therefore far.

While the number of identifiers shown to significantly change in phosphorylation in WT cells following Rap treatment mirrored previous studies (Fig. 2b) (Werth *et al.*, 2019), *vip1-1* yielded a larger change in phosphopeptide abundance following TOR inhibition than the WT (Fig. 2a). However, the number of identifiers found to be differentially phosphorylated was significantly lower when comparing WT and *vip1-1* before (1625 identifiers) and after (346 identifiers) TOR inhibition (Fig. 2c,d). These results strongly suggested that TOR kinase and PP-InsPs operated in the same signalling cascade in agreement with their previously observed genetic interaction (Couso *et al.*, 2016). We cannot disregard that they could directly interact, as we found an upregulation of S2598 on TOR in *vip1-1* after Rap treatment (Table S3) when TOR activity is faster inhibited in the mutant (Fig. 1a–c). Previously, this phosphosite was identified in

Chlamydomonas WT, but no change was detected in response to different TOR inhibitors (AZD8055, Torin 1 and Rap) (Werth *et al.*, 2019). Our results suggest TOR phosphorylation at S2598 may be regulated by PP-InsPs, although the impact on TOR activity is still unknown.

We also identified a novel connection between PP-InsPs and established processes under TOR control (Table S3). Autophagy is inhibited by active TOR signalling in diverse eukaryotes including algae and plants (Díaz-Troya *et al.*, 2008; Yu *et al.*, 2018). Recently, VIP1 has also been connected to the regulation of autophagy by modulating the level of ATG proteins in *Candida albicans* (Ma *et al.*, 2020). We found an overaccumulation of lipidated ATG8, therefore indicating an overactivation of the recycling process of autophagy in *vip1-1* under Rap conditions (Pérez-Pérez *et al.*, 2010) (Fig. 1d). We also found an ATG11 phosphosite (ATG11-S1176) (Table S3) that was significantly downregulated in *vip1-1* under control conditions. ATG11 is a well known scaffold protein that interacts with phosphorylated ATG29 or ATG32 in yeasts to induce mitophagy and the organisation of the phagophore assembly site (Aoki *et al.*, 2011; Mao *et al.*, 2013) and encourages starvation-induced phosphorylation of ATG1 in Arabidopsis, a downstream TOR target (Li *et al.*, 2014). Taking these results together, we conclude that autophagy is regulated coordinately with TOR and PP-InsPs signalling pathways in *Chlamydomonas*, but that PP-InsPs may also act independently of TOR to potentiate this recycling process.

LARP1 proteins are direct effectors of mTORC1 in mediating mRNA translation (Thoreen *et al.*, 2012) and are found in many eukaryotes (Deragon & Bousquet-Antonelli, 2015). However, none of the significantly changing phosphorylated identifiers found in *Chlamydomonas* LARP1 (Table S3) was conserved in yeasts or humans. AtLARP1 showed significantly decreased phosphorylation on S644 and S649 following TOR inhibition (Van Leene *et al.*, 2019); the former is conserved in *Chlamydomonas* (LARP1-S810) and identified as a phosphosite in Werth *et al.* (2017), but did not significantly change following TOR inhibition (Werth *et al.*, 2019). However, LARP1-S817 phosphorylation decreased following TOR inhibition in the same study (Werth *et al.*, 2019), which was also observed here in WT after Rap inhibition however no significant differences were seen in *vip1-1* (Table S3). Instead, three different phosphosites were significantly decreased in *vip1-1* compared with WT (LARP1-S529, -T668 and -S670) and only -S670 was upregulated after Rap treatment (Table S3). These results suggest that PP-InsPs act partly through the TOR signalling cascade and partly through TORC1-independent mechanisms to effect LARP1 phosphorylation.

PP-InsPs and TOR control phosphorylation of photosynthetic apparatus

Gene ontology analysis revealed an unexpected enrichment of photosynthetic targets (Fig. 3) that were not described in previous studies reporting protein phosphorylation patterns under TOR inhibition in either *Chlamydomonas* or *Arabidopsis* (Roustan & Weckwerth, 2018; Van Leene *et al.*, 2019; Werth *et al.*, 2019).

However, proteomic analysis of reversible cysteine oxidation, a PTM known to crosstalk with phosphorylation, indicated that photosynthesis is regulated by TOR in *Chlamydomonas* (Ford *et al.*, 2019). Similarly, our data here showed significant differences in photosynthesis-related proteins in global and phosphoproteomic data between WT and *vip1-1* under control conditions (Tables S4, S5). These results indicated reduced levels of the catalytic subunits D1 and D2 and reaction centres psbC (CP43) and psbB (CP47). Also, psbC-S456 and psbB-T501 were highly downregulated in the mutant under control conditions but not after Rap treatment (Table S5). D1, D2 and psbC are primarily phosphorylated in response to light stress and endogenous circadian rhythm at their N-terminal threonine residues (Elich *et al.*, 1992; Booi-James *et al.*, 2002) by the Ser/Thr kinase STATE TRANSITION8 (STN8) (Bonardi *et al.*, 2005; Vainonen *et al.*, 2005; Rochaix *et al.*, 2012). The *Chlamydomonas* paralogue of STN8, STL1 (Cre12.g483650.t1.2) showed a significant downregulation on T126 in *vip1-1* that was compensated in the presence of Rap (Table S5). Although this kinase is regulated by the redox state of the PQ pool (Bennett, 1991; Fristedt *et al.*, 2009), it has also been reported to be subjected to phosphorylation (Reiland *et al.*, 2011). Additionally, STL1-T126 was previously reported in *Chlamydomonas* (Bergner *et al.*, 2015). The phosphorylation of PSII core proteins is part of the PSII repair cycle that proceeds before the proteolytic degradation of damaged D1 protein, preventing its degradation by proteases (Koivuniemi *et al.*, 1995). Additionally, STN8 is thought to control the transitions from linear to CEF by controlling the phosphorylation of PGRL1 in *Arabidopsis* (Reiland *et al.*, 2011). Our data could indicate that the downregulation of D1 found in *vip1-1* is a consequence of the differential phosphorylated identifiers in STL1 and core components found in this mutant and that PP-InsPs and TOR act coordinately upstream of this process controlling PSII photochemistry, possibly facilitating the transition between linear and CEF under high irradiances.

We also determined the light harvesting antenna protein LHCBM5 (Cre03.g156900.t1.2) has decreased abundance in *vip1-1*. Although LHCBM5 has no homologue in plants, it has been suggested that this protein plays a similar role to the CP24 protein in *Arabidopsis* (Takahashi *et al.*, 2006). CP24-deficient plants displayed altered kinetics of state transitions (Kovács *et al.*, 2006). The downregulation of LHCBM5 detected in the *vip1-1* mutant could link PP-InsPs to state transitions in *Chlamydomonas* as LHCBM5 is the more abundant LHCB (type II) polypeptide found in PSI-LHCI under state 2 (Takahashi *et al.*, 2006).

Phosphorylation of LHCB4 and LHCB5 (CP26) is considered fundamental for the detachment of LHCBM polypeptides from PSII during the transition from state 1 to state 2 (Iwai *et al.*, 2008). Three identifiers belonging to LHCB4 (T11, T17 and S39) were significantly downregulated in the mutant under control conditions. LHCB4-T7 and T11 have been previously found to be connected with the phosphorylation state of LHCSR3 that is involved in photoprotective NPQ in *Chlamydomonas* (Scholz *et al.*, 2019). Another identifier found in this study, LHCB4-S103 (Table S5), has been previously linked to kinase STT7

activity in this alga (Bergner *et al.*, 2015), but we could not find any significant difference in the conditions tested. We also found four identifiers in LHCB5 (T10, -S63, -T187, -S202) (Table S5), although S63 was the only one significantly changing in *vip1-1* under control conditions. The upregulation of S63 was then prevented after Rap treatment indicating that TOR and PP-InsPs share this target. Also, LHCB5-T10 has previously been identified after mapping *in vivo* phosphorylation sites in integral and peripheral membrane proteins (Vener, 2007). These data suggest that PP-InsPs and TOR control state transitions at different levels, with LHCBM5 protein abundance and the phosphorylation state of LHCB4 and LHCB5 influencing the transition to state 2 when light compensation mechanisms are required. Additionally, repair-specific proteins (VIPP1 and CDJ2) were upregulated in *vip1-1* mutant. In *Chlamydomonas*, *vipp1* amiRNA knockdown strains are sensitive to HL, which is likely to be due to structural defects in PSII (Nordhues *et al.*, 2012). The upregulation of this protein in *vip1-1* suggests that PSII repair mechanisms are more active in this mutant, and are likely to be as a consequence of PSII malfunction. This is supported by decreased F_v/F_m (Table 1) and ETR II (Fig. 4b) values detected in the mutant.

PP-InsPs and TOR are involved in the maintenance of cell energy levels

In *Arabidopsis*, PGRL1-T62-T63 has been reported to be a possible target of STN8 kinase (Reiland *et al.*, 2011). We found one identifier in PGRL1 (S50) to be downregulated in *vip1-1* under control conditions and in WT after Rap treatment. The levels of PGRL1-S50 were alleviated in the presence of Rap, but only in the mutant, therefore indicating a fine modulation mediated by PP-InsPs and TOR that correlates to the tight control of the initiation of CEF mediated by PGRL1 (Johnson *et al.*, 2014).

Under stress, CEF provides ATP for CO₂ fixation (Lucker & Kramer, 2013), balances overreduction of PSI, and readjusts the ATP poise, leading to increased lumen acidification that is important for photoprotection (Alric, 2010; Peltier *et al.*, 2010; Leister & Shikanai, 2013; Shikanai, 2014). ATP synthase subunits E and II are increased in *vip1-1* (Table S1) that corresponds with the high ATP levels found in this mutant (Fig. 5c). Although PP-InsPs have been previously linked to the control of intracellular ATP in yeast *kcs1Δ* mutants (Szjgyarto *et al.*, 2011), *vip1* mutants have not previously been directly connected with this phenotype. While no IP6K homologue is found in algae or plants, the detection of InsP₈ (1,5(PP)₂-InsP₄) suggests the presence of a functional IP6K enzyme (Desai *et al.*, 2014; Laha *et al.*, 2015; Couso *et al.*, 2016), or a noncanonical ITPK function (Cridland & Gillaspay, 2020) that could be regulating ATP levels in coordination with VIP1. Recently, VIP1 was also reported to have a bifunctional kinase/pyrophosphatase activity that produces and destroys 1-PP-InsPs at the expense of consuming ATP in yeast (Dollins *et al.*, 2020). This could contribute to the increase in ATP observed in the *Chlamydomonas vip1-1* mutant. Additionally, mTOR is a homeostatic ATP sensor that adjusts ribosome biogenesis to ATP intracellular levels (Dennis, 2001).

Although *vip1-1* displays higher ATP levels than WT, we did not detect any difference in TOR activity before Rap treatment, suggesting that this activation pathway may not be conserved in this alga.

NPQ, PP-InsPs and TOR coordinate to protect cells to excessive irradiance

The photoprotective process NPQ is activated in almost all photosynthetic organisms in PSII antenna to dissipate excess light as heat (Ruban, 2016). NPQ is catalysed by Light Harvesting Complex Stress Related (LHCSR) subunits, with a major role observed for LHCSR3 (Girolomoni *et al.*, 2019). We found three identifiers of LHCSR3 (-S165, -T161, -Y170) (Table S5) increased in *vip1-1* and only Y170 remained upregulated in the presence of Rap. LHCSR3 phosphorylation has also been reported as nonessential for NPQ activation in *Chlamydomonas* (Bonente *et al.*, 2011). However, that work compared phosphorylated with dephosphorylated LHCSR3 that contrasts with the over-phosphorylated identifiers found in *vip1-1*. Protein levels of LHCSR3 have previously been connected to the regulation of NPQ (Peers *et al.*, 2009) but we could not detect any significant difference in *vip1-1* compared with WT (Table S4), suggesting that PP-InsPs and possibly TOR are regulating NPQ at post-translational level. LHCSR3 phosphorylation at the N-terminus (-S26, -S28-T32 and -T33) has been reported to operate as a molecular switch modulating LHCB4 phosphorylation, which in turn is important for PSII-LHCII disassembly before state transitions (Bergner *et al.*, 2015; Scholz *et al.*, 2019). Also, Arabidopsis *koLhcb4* mutants present lower activation of NPQ (de Bianchi *et al.*, 2011). These results indicated a tight control of photoprotective mechanisms mediated by PP-InsPs that act independently (-Y170) and coordinately with TOR (-S165, -T161) over the phosphorylation of LHCSR3. We also need to consider that the deregulation of LHCB4 (CP29) phosphorylation in *vip1-1* is suggesting that NPQ is finely controlled by PP-InsPs at different levels in the photosynthetic machinery. *In vivo* measurements of NPQ levels in the WT, *vip1-1*, and complemented line revealed highly decreased NPQ levels after HL in *vip1-1* that were not observed following Rap treatment (Figs 5d, 6a). Although NPQ does not seem to be affected by TOR inhibition in any of the strains, we cannot disregard that LHCSR3-S165 and -T161 levels were compensated after Rap treatment (Table S5). This is another example of the multiplex regulation mediated by PP-InsPs and TOR kinase over the same targets that are mechanistically difficult to delineate.

Nonphotochemical quenching, InsP₇, and InsP₈ levels were also compared among WT, *vip1-1* and the NPQ defective mutant *npq2*. We found an important decrease of PP-InsPs in *npq2* that does not respond to Rap treatment (Fig. 6b,c). These data indicated a possible feedback loop in the regulation of NPQ and PP-InsPs biosynthesis that is independent of TOR signalling (Fig. 6b,c). We also found that PP-InsPs levels and NPQ were highly different from WT levels under HL conditions, indicating that this feedback regulation may be especially relevant under stress conditions where NPQ is activated.

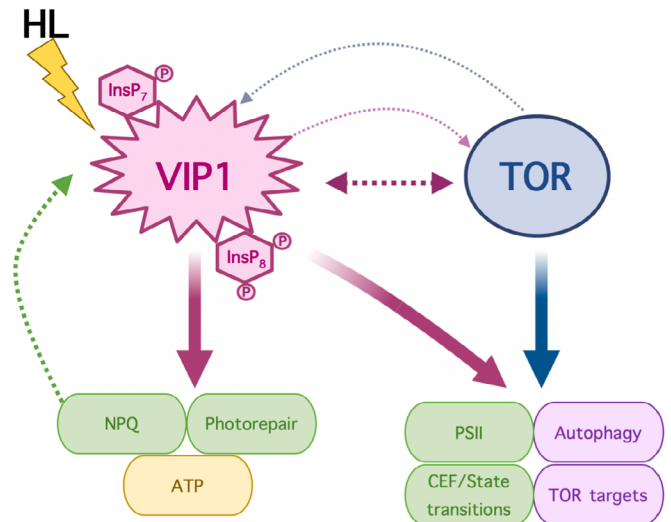


Fig. 7 Summary figure of proposed relationships between target of rapamycin (TOR), and pyro-inositol polyphosphates (PP-InsPs), inositol polyphosphate-7 (InsP₇) and inositol polyphosphate-8 (InsP₈) produced by VIP1 and processes that are under their influence found in this study. PP-InsPs/VIP1 can directly regulate high light stress and energy levels (on the left) but they also coordinate with TOR (on the right) in regulating photosynthesis and previously known TOR targets such as autophagy. Dashed arrow indicates that PP-InsPs/VIP1 and TOR have a complex interaction that rebound TOR kinase activity and InsPs biosynthesis. Under favourable conditions, VIP is proposed to stimulate TOR kinase activity and TOR is proposed to stimulate PP-InsPs biosynthesis catalysed by VIP. Our data also indicate that complex feedback loops may be regulating PP-InsPs outside TOR signalling such as in nonphotochemical quenching (NPQ).

Conclusion

Overall, our data indicated a strong relationship between TOR kinase and VIP1/PP-InsPs that impacted autophagy and TOR activity in *Chlamydomonas*. We have uncovered that PP-InsPs share common targets with TOR in controlling photosynthetic machinery and compensation mechanisms including state transitions and CEF (Fig. 7). We have also identified PP-InsPs as key components of the signal transduction machinery that can act independently of TOR controlling NPQ under high irradiance or energy levels (Fig. 7). We have begun unravelling the influence of these essential signalling compounds in *Chlamydomonas*' PTMs; however, several questions still remain. Future work should address the role of PP-InsP signalling in specific cell compartments as well as the conditions in which PP-InsPs signal transduction act independently and/or coordinately with TOR signalling over different targets to maintain cell homeostasis.

Acknowledgements







This research was supported by the Ministerio de Economía y Competitividad (grant PGC2018-099048-B-100) to JLC. During this time, IC was a recipient of the MSCA-IF-EF-RI contract (grant no. 750996) from the European Commission and Beatriz Galindo Fellowship from the Ministerio de Educación y Formación Profesional. This work was supported by a National

Science Foundation CAREER award (MCB-1552522) to LMH and by National Science Foundation Grant (MCB-1616820) to JGU. The authors declare that they have no conflict of interest

Author contributions

IC, LMH, JGU and JLC contributed to planning and experimental design; IC, MMF and ALS performed experiments and data analysis; and IC, MMF, ALS, LMH and JLC wrote the manuscript.

ORCID

Inmaculada Couso  <https://orcid.org/0000-0003-2849-675X>
 José L. Crespo  <https://orcid.org/0000-0003-3514-1025>
 Megan M. Ford  <https://orcid.org/0000-0003-4468-1891>
 Leslie M. Hicks  <https://orcid.org/0000-0002-8008-3998>
 Amanda L. Smythers  <https://orcid.org/0000-0002-1552-6705>
 James G. Umen  <https://orcid.org/0000-0003-4094-9045>

Data availability

The data that support the findings of this study are openly available in the ProteomeXchange Consortium via the PRIDE partner repository and can be accessed with the Identifier PXD023085.

References

- Albert V, Hall MN. 2014. mTOR signaling in cellular and organismal energetics. *Current Opinion in Cell Biology* 33: 55–66.
- Alric J. 2010. Cyclic electron flow around photosystem I in unicellular green algae. *Photosynthesis Research* 106: 47–56.
- Aoki Y, Kanki T, Hirota Y, Kurihara Y, Saigusa T, Uchiumi T, Kang D. 2011. Phosphorylation of serine 114 on Atg32 mediates mitophagy. *Molecular Biology of the Cell* 22: 3206–3217.
- Ashburner M, Ball CA, Blake JA, Botstein D, Butler H, Cherry JM, Davis AP, Dolinski K, Dwight SS, Eppig JT *et al.* 2000. Gene Ontology: tool for the unification of biology. *Nature Genetics* 25: 25–29.
- Bennett J. 1991. Protein phosphorylation in green plant chloroplasts. *Annual Review of Plant Physiology and Plant Molecular Biology* 42: 281–311.
- Bergner SV, Scholz M, Trompelt K, Barth J, Gäbelein P, Steinbeck J, Xue H, Clowes S, Fucile G, Goldschmidt-Clermont M *et al.* 2015. STATE TRANSITION7-dependent phosphorylation is modulated by changing environmental conditions, and its absence triggers remodeling of photosynthetic protein complexes. *Plant Physiology* 168: 615–634.
- Bhandari R, Saiardi A, Ahmadibeni Y, Snowman AM, Resnick AC, Kristiansen TZ, Molina H, Pandey A, Werner JK, Juluri KR *et al.* 2007. Protein pyrophosphorylation by inositol pyrophosphates is a posttranslational event. *Proceedings of the National Academy of Sciences, USA* 104: 15305–15310.
- de Bianchi S, Betterle N, Kouril R, Cazzaniga S, Boekema E, Bassi R, Dall'Osto L. 2011. *Arabidopsis* mutants deleted in the light-harvesting protein LHCB4 have a disrupted photosystem II macrostructure and are defective in photoprotection. *Plant Cell* 23: 2659–2679.
- Bonardi V, Pesaresi P, Becker T, Schleiff E, Wagner R, Pfanschmidt T, Jahns P, Leister D. 2005. Photosystem II core phosphorylation and photosynthetic acclimation require two different protein kinases. *Nature* 437: 1179–1182.
- Bonente G, Ballottari M, Truong TB, Morosinotto T, Ahn TK, Fleming GR, Niyogi KK, Bassi R. 2011. Analysis of LHCSR3, a protein essential for feedback de-excitation in the green alga *Chlamydomonas reinhardtii*. *PLoS Biology* 9: e1000577.
- Booij-James IS, Swegle WM, Edelman M, Mattoo AK. 2002. Phosphorylation of the D1 photosystem II reaction center protein is controlled by an endogenous circadian rhythm. *Plant Physiology* 130: 2069–2075.
- Caldana C, Martins MCM, Mubeen U, Urrea-Castellanos R. 2019. The magic 'hammer' of TOR: the multiple faces of a single pathway in the metabolic regulation of plant growth and development. *Journal of Experimental Botany* 70: 2217–2225.
- Cardol P, Alric J, Girard-Bascou J, Franck F, Wollman F-A, Finazzi G. 2009. Impaired respiration discloses the physiological significance of state transitions in *Chlamydomonas*. *Proceedings of the National Academy of Sciences, USA* 106: 15979–15984.
- Chaux F, Johnson X, Auroy P, Beyly-Adriano A, Te I, Cuié S, Peltier G. 2017. PGRL1 and LHCSR3 compensate for each other in controlling photosynthesis and avoiding photosystem I photoinhibition during high light acclimation of *Chlamydomonas* cells. *Molecular Plant* 10: 216–218.
- Couso I, Evans BS, Li J, Liu Y, Ma F, Diamond S, Allen DK, Umen JG. 2016. Synergism between inositol polyphosphates and TOR kinase signaling in nutrient sensing, growth control, and lipid metabolism in *Chlamydomonas*. *Plant Cell* 28: 2026–2042.
- Couso I, Pérez-Pérez ME, Ford MM, Martínez-Force E, Hicks LM, Umen JG, Crespo JL. 2020. Phosphorus availability regulates torc1 signaling via LST8 in *Chlamydomonas*. *Plant Cell* 32: 69–80.
- Couso I, Pérez-Pérez ME, Martínez-Force E, Kim HS, He Y, Umen JG, Crespo JL. 2018. Autophagic flux is required for the synthesis of triacylglycerols and ribosomal protein turnover in *Chlamydomonas*. *Journal of Experimental Botany* 69: 1355–1367.
- Crespo JL, Díaz-Troya S, Florencio FJ. 2005. Inhibition of target of rapamycin signaling by rapamycin in the unicellular green alga *Chlamydomonas reinhardtii*. *Plant Physiology* 139: 1736–1749.
- Cridland C, Gillaspay G. 2020. Inositol pyrophosphate pathways and mechanisms: what can we learn from plants? *Molecules* 25: 2789.
- Dennis PB. 2001. Mammalian TOR: a homeostatic ATP sensor. *Science* 294: 1102–1105.
- Deragon J-M, Bousquet-Antonelli C. 2015. The role of LARP1 in translation and beyond. *Wiley Interdisciplinary Reviews: RNA* 6: 399–417.
- Desai M, Rangarajan P, Donahue JL, Williams SP, Land ES, Mandal MK, Phillippy BQ, Perera IY, Raboy V, Gillaspay GE. 2014. Two inositol hexakisphosphate kinases drive inositol pyrophosphate synthesis in plants. *The Plant Journal* 80: 642–653.
- Díaz-Troya S, Pérez-Pérez ME, Florencio FJ, Crespo JL. 2008. The role of TOR in autophagy regulation from yeast to plants and mammals. *Autophagy* 4: 851–865.
- Dobrenel T, Caldana C, Hanson J, Robaglia C, Vincenz M, Veit B, Meyer C. 2016. TOR signaling and nutrient sensing. *Annual Review of Plant Biology* 67: 261–285.
- Dollins DE, Bai W, Fridy PC, Otto JC, Neubauer JL, Gattis SG, Mehta KPM, York JD. 2020. Vip1 is a kinase and pyrophosphatase switch that regulates inositol diphosphate signaling. *Proceedings of the National Academy of Sciences, USA* 117: 9356–9364.
- Elich TD, Edelman M, Mattoo AK. 1992. Identification, characterization, and resolution of the in vivo phosphorylated form of the D1 photosystem II reaction center protein. *The Journal of Biological Chemistry* 267: 3523–3529.
- Finazzi G, Furia A, Barbagallo RP, Forti G. 1999. State transitions, cyclic and linear electron transport and photophosphorylation in *Chlamydomonas reinhardtii*. *Biochimica et Biophysica Acta (BBA) – Bioenergetics* 1413: 117–129.
- Fonseca BD, Zakaria C, Jia J-J, Graber TE, Svitkin Y, Tahmasebi S, Healy D, Hoang H-D, Jensen JM, Diaio IT *et al.* 2015. La-related protein 1 (LARP1) represses terminal oligopyrimidine (TOP) mRNA translation downstream of mTOR Complex 1 (mTORC1). *Journal of Biological Chemistry* 290: 15996–16020.
- Ford MM, Smythers AL, McConnell EW, Lowery SC, Kolling DRJ, Hicks LM. 2019. Inhibition of TOR in *Chlamydomonas reinhardtii* leads to rapid cysteine oxidation reflecting sustained physiological changes. *Cells* 8: 1171.
- Fristedt R, Willig A, Granath P, Crèvecoeur M, Rochoix J-D, Vener AV. 2009. Phosphorylation of photosystem II controls functional macroscopic folding of photosynthetic membranes in *Arabidopsis*. *Plant Cell* 21: 3950–3964.

- Gerasimaite R, Pavlovic I, Capolicchio S, Hofer A, Schmidt A, Jessen HJ, Mayer A. 2017. Inositol pyrophosphate specificity of the SPX-dependent polyphosphate polymerase VTC. *ACS Chemical Biology* 12: 648–653.
- Girolomoni L, Cazzaniga S, Pinnola A, Perozeni F, Ballottari M, Bassi R. 2019. LHCSR3 is a nonphotochemical quencher of both photosystems in *Chlamydomonas reinhardtii*. *Proceedings of the National Academy of Sciences, USA* 116: 4212–4217.
- Goldschmidt-Clermont M, Bassi R. 2015. Sharing light between two photosystems: mechanism of state transitions. *Current Opinion in Plant Biology* 25: 71–78.
- González A, Hall MN. 2017. Nutrient sensing and TOR signaling in yeast and mammals. *EMBO Journal* 36: 397–408.
- Gupta TK, Klumpe S, Gries K, Heinz S, Wietrzynski W, Ohnishi N, Niemeyer J, Spaniol B, Schaffer M, Rast A *et al.* 2021. Structural basis for VIPP1 oligomerization and maintenance of thylakoid membrane integrity. *Cell* 184: 3643–3659.e23.
- Hahn A, Vonck J, Mills DJ, Meier T, Kühlbrandt W. 2018. Structure, mechanism, and regulation of the chloroplast ATP synthase. *Science* 360: eaat4318.
- Iwai M, Takahashi Y, Minagawa J. 2008. Molecular remodeling of photosystem II during state transitions in *Chlamydomonas reinhardtii*. *Plant Cell* 20: 2177–2189.
- Iwai M, Takizawa K, Tokutsu R, Okamuro A, Takahashi Y, Minagawa J. 2010. Isolation of the elusive supercomplex that drives cyclic electron flow in photosynthesis. *Nature* 464: 1210–1213.
- Johnson X, Steinbeck J, Dent RM, Takahashi H, Richaud P, Ozawa S-I, Houille-Vernes L, Petroustos D, Rappaport F, Grossman AR *et al.* 2014. Proton gradient regulation 5-mediated cyclic electron flow under ATP- or redox-limited conditions: a study of $\Delta atpase pgr5$ and $\Delta rbcL pgr5$ mutants in the green alga *Chlamydomonas reinhardtii*. *Plant Physiology* 165: 438–452.
- Jung JY, Ried MK, Hothorn M, Poirier Y. 2018. Control of plant phosphate homeostasis by inositol pyrophosphates and the SPX domain. *Current Opinion in Biotechnology* 49: 156–162.
- Kang SA, Pacold ME, Cervantes CL, Lim D, Lou HJ, Ottina K, Gray NS, Turk BE, Yaffe MB, Sabatini DM. 2013. mTORC1 phosphorylation sites encode their sensitivity to starvation and rapamycin. *Science* 341: 1236566.
- Klughammer C, Schreiber U. 2008. Complementary PS II quantum yields calculated from simple fluorescence parameters measured by PAM fluorometry and the Saturation Pulse method. *PAM Application Notes* 1: 27–35.
- Koivuniemi A, Aro E-M, Andersson B. 1995. Degradation of the D1- and D2-proteins of photosystem II in higher plants is regulated by reversible phosphorylation. *Biochemistry* 34: 16022–16029.
- Kovács L, Damkjær J, Kereiche S, Iliaoaia C, Ruban AV, Boekema EJ, Jansson S, Horton P. 2006. Lack of the light-harvesting complex CP24 affects the structure and function of the grana membranes of higher plant chloroplasts. *Plant Cell* 18: 3106–3120.
- Kramer DM, Johnson G, Kiirats O, Edwards GE. 2004. New fluorescence parameters for the determination of Q a redox state and excitation energy fluxes. *Photosynthesis Research* 79: 209–218.
- Kress E, Jahns P. 2017. The dynamics of energy dissipation and xanthophyll conversion in *Arabidopsis* indicate an indirect photoprotective role of zeaxanthin in slowly inducible and relaxing components of non-photochemical quenching of excitation energy. *Frontiers in Plant Science* 8: 2094.
- Laha D, Johnen P, Azevedo C, Dyrnowski M, Weiß M, Capolicchio S, Mao H, Iven T, Steenbergen M, Freyer M *et al.* 2015. VIH2 regulates the synthesis of inositol pyrophosphate insp 8 and jasmonate-dependent defenses in *Arabidopsis*. *Plant Cell* 27: 1082–1097.
- Leister D, Shikanai T. 2013. Complexities and protein complexes in the antimycin A-sensitive pathway of cyclic electron flow in plants. *Frontiers in Plant Science* 4: 161.
- Lemaire C, Wollman FA. 1989. The chloroplast ATP synthase in *Chlamydomonas reinhardtii*. I. Characterization of its nine constitutive subunits. *The Journal of Biological Chemistry* 264: 10228–10234.
- Lemeille S, Turkina MV, Vener AV, Rochaix J-D. 2010. STT7-dependent phosphorylation during state transitions in the green alga *Chlamydomonas reinhardtii*. *Molecular & Cellular Proteomics* 9: 1281–1295.
- Li F, Chung T, Vierstra RD. 2014. AUTOPHAGY-RELATED11 plays a critical role in general autophagy- and senescence-induced mitophagy in *Arabidopsis*. *Plant Cell* 26: 788–807.
- Li X, Gu C, Hostachy S, Sahu S, Wittwer C, Jessen HJ, Fiedler D, Wang H, Shears SB. 2020. Control of XPR1-dependent cellular phosphate efflux by InsP8 is an exemplar for functionally-exclusive inositol pyrophosphate signaling. *Proceedings of the National Academy of Sciences, USA* 117: 3568–3574.
- Liu C, Willmund F, Whitelegge JP, Hawat S, Knapp B, Lodha M, Schroda M. 2005. J-domain protein CDJ2 and HSP70B are a plastidic chaperone pair that interacts with vesicle-inducing protein in plastids 1. *Molecular Biology of the Cell* 16: 1165–1177.
- Livermore TM, Azevedo C, Kolozsvari B, Wilson MSC, Saiardi A. 2016. Phosphate, inositol and polyphosphates. *Biochemical Society Transactions* 44: 253–259.
- Loewith R, Hall MN. 2011. Target of rapamycin (TOR) in nutrient signaling and growth control. *Genetics* 189: 1177–1201.
- Lucker B, Kramer DM. 2013. Regulation of cyclic electron flow in *Chlamydomonas reinhardtii* under fluctuating carbon availability. *Photosynthesis Research* 117: 449–459.
- Lunn JE, Feil R, Hendriks JHM, Gibon Y, Morcuende R, Osuna D, Scheible W-R, Carillo P, Hajirezaei M-R, Stitt M. 2006. Sugar-induced increases in trehalose 6-phosphate are correlated with redox activation of ADP-glucose pyrophosphorylase and higher rates of starch synthesis in *Arabidopsis thaliana*. *Biochemical Journal* 397: 139–148.
- Ma T, Yu Q, Ma C, Mao X, Liu Y, Peng X, Li M. 2020. Role of the inositol polyphosphate kinase VIP1 in autophagy and pathogenesis in *Candida albicans*. *Future Microbiology* 15: 1363–1377.
- Mao K, Chew LH, Inoue-Aono Y, Cheong H, Nair U, Popelka H, Yip CK, Klionsky DJ. 2013. ATG29 phosphorylation regulates coordination of the ATG17-ATG31-ATG29 complex with the ATG11 scaffold during autophagy initiation. *Proceedings of the National Academy of Sciences, USA* 110: E2875–E2884.
- Mulugu S, Bai W, Fridy PC, Bastidas RJ, Otto JC, Dollins DE, Haystead TA, Ribeiro AA, York JD. 2007. A conserved family of enzymes that phosphorylate inositol hexakisphosphate. *Science* 316: 106–109.
- Niyogi KK, Björkman O, Grossman AR. 1997. *Chlamydomonas* xanthophyll cycle mutants identified by video imaging of chlorophyll fluorescence quenching. *Plant Cell* 9: 1369–1380.
- Niyogi KK, Grossman AR, Björkman O. 1998. Arabidopsis mutants define a central role for the xanthophyll cycle in the regulation of photosynthetic energy conversion. *Plant Cell* 10: 1121–1134.
- Nordhues A, Schöttler MA, Unger A-K, Geimer S, Schönfelder S, Schmollinger S, Rütgers M, Finazzi G, Soppa B, Sommer F *et al.* 2012. Evidence for a role of VIPP1 in the structural organization of the photosynthetic apparatus in *Chlamydomonas*. *Plant Cell* 24: 637–659.
- Peers G, Truong TB, Ostendorf E, Busch A, Elrad D, Grossman AR, Hippler M, Niyogi KK. 2009. An ancient light-harvesting protein is critical for the regulation of algal photosynthesis. *Nature* 462: 518–521.
- Peltier G, Tolleter D, Billon E, Cournac L. 2010. Auxiliary electron transport pathways in chloroplasts of microalgae. *Photosynthesis Research* 106: 19–31.
- Pérez-Pérez ME, Couso I, Crespo JL. 2017. The TOR signaling network in the model unicellular green alga *Chlamydomonas reinhardtii*. *Biomolecules* 7: 54.
- Pérez-Pérez ME, Florencio FJ, Crespo JL. 2010. Inhibition of target of rapamycin signaling and stress activate autophagy in *Chlamydomonas reinhardtii*. *Plant Physiology* 152: 1874–1888.
- Philippe L, van den Elzen AMG, Watson MJ, Thoreen CC. 2020. Global analysis of LARP1 translation targets reveals tunable and dynamic features of 5' TOP motifs. *Proceedings of the National Academy of Sciences, USA* 117: 5319–5328.
- Reiland S, Finazzi G, Endler A, Willig A, Baerenfaller K, Grossmann J, Gerrits B, Rutishauser D, Grussem W, Rochaix J-D *et al.* 2011. Comparative phosphoproteome profiling reveals a function of the STN8 kinase in fine-tuning of cyclic electron flow (CEF). *Proceedings of the National Academy of Sciences, USA* 108: 12955–12960.
- Richter ML, Hein R, Huchzermeyer B. 2000. Important subunit interactions in the chloroplast ATP synthase. *Biochimica et Biophysica Acta (BBA) – Bioenergetics* 1458: 326–342.

- Ried MK, Wild R, Zhu J, Pipercevic J, Sturm K, Broger L, Harmel RK, Abriata LA, Hothorn LA, Fiedler D *et al.* 2021. Inositol pyrophosphates promote the interaction of SPX domains with the coiled-coil motif of PHR transcription factors to regulate plant phosphate homeostasis. *Nature Communications* 12: 384.
- Robitaille AM, Christen S, Shimobayashi M, Cornu M, Fava LL, Moes S, Prescianotto-Baschong C, Sauer U, Jenoe P, Hall MN. 2013. Quantitative phosphoproteomics reveal mTORC1 activates de novo pyrimidine synthesis. *Science* 339: 1320–1323.
- Rochaix J-D, Lemeille S, Shapiguzov A, Samol I, Fucile G, Willig A, Goldschmidt-Clermont M. 2012. Protein kinases and phosphatases involved in the acclimation of the photosynthetic apparatus to a changing light environment. *Philosophical Transactions of the Royal Society of London. Series B: Biological Sciences* 367: 3466–3474.
- Roustan V, Weckwerth W. 2018. Quantitative phosphoproteomic and system-level analysis of tor inhibition unravel distinct organellar acclimation in *Chlamydomonas reinhardtii*. *Frontiers in Plant Science* 9: 1590.
- Ruban AV. 2016. Nonphotochemical chlorophyll fluorescence quenching: mechanism and effectiveness in protecting plants from photodamage. *Plant Physiology* 170: 1903–1916.
- Sager R. 1955. Inheritance in the green alga *Chlamydomonas reinhardtii*. *Genetics* 40: 476–489.
- Saiardi A. 2004. Phosphorylation of proteins by inositol pyrophosphates. *Science* 306: 2101–2105.
- Saiardi A. 2012a. How inositol pyrophosphates control cellular phosphate homeostasis? *Advances in Biological Regulation* 52: 351–359.
- Saiardi A. 2012b. Cell signalling by inositol pyrophosphates. In: Balla T, Wymann M, York J, eds. *Phosphoinositides II: the diverse biological functions*. Subcellular biochemistry, vol. 59. Dordrecht, the Netherlands: Springer, 413–443.
- Saiardi A. 2016. Protein pyrophosphorylation: moving forward. *Biochemical Journal* 473: 3765–3768.
- Saiardi A, Erdjument-Bromage H, Snowman AM, Tempst P, Snyder SH. 1999. Synthesis of diphosphoinositol pentakisphosphate by a newly identified family of higher inositol polyphosphate kinases. *Current Biology* 9: 1323–1326.
- Scarpin MR, Leiboff S, Brunkard JO. 2020. Parallel global profiling of plant TOR dynamics reveals a conserved role for LARP1 in translation. *eLife* 9: e58795.
- Schepetilnikov M, Ryabova LA. 2018. Recent discoveries on the role of TOR (target of rapamycin) signaling in translation in plants. *Plant Physiology* 176: 1095–1105.
- Scholz M, Gäbelein P, Xue H, Mosebach L, Bergner SV, Hippler M. 2019. Light-dependent N-terminal phosphorylation of LHCSR3 and LHCB4 are interlinked in *Chlamydomonas reinhardtii*. *The Plant Journal* 99: 877–894.
- Secco D, Wang C, Arpat BA, Wang Z, Poirier Y, Tyerman SD, Wu P, Shou H, Whelan J. 2012. The emerging importance of the SPX domain-containing proteins in phosphate homeostasis. *New Phytologist* 193: 842–851.
- Shears SB. 2015. Inositol pyrophosphates: why so many phosphates? *Advances in Biological Regulation* 57: 203–216.
- Shears SB, Wang H. 2019. Inositol phosphate kinases: expanding the biological significance of the universal core of the protein kinase fold. *Advances in Biological Regulation* 71: 118–127.
- Shi L, Wu Y, Sheen J. 2018. TOR signaling in plants: conservation and innovation. *Development* 145: dev160887.
- Shikanai T. 2014. Central role of cyclic electron transport around photosystem I in the regulation of photosynthesis. *Current Opinion in Biotechnology* 26: 25–30.
- Soulard A, Cremonesi A, Moes S, Schütz F, Jenö P, Hall MN. 2010. The rapamycin-sensitive phosphoproteome reveals that tor controls protein kinase A toward some but not all substrates. *Molecular Biology of the Cell* 21: 3475–3486.
- Sun L-L, Li M, Suo F, Liu X-M, Shen E-Z, Yang B, Dong M-Q, He W-Z, Du L-L. 2013. Global analysis of fission yeast mating genes reveals new autophagy factors. *PLoS Genetics* 9: e1003715.
- Szjgyarto Z, Garede A, Azevedo C, Saiardi A. 2011. Influence of inositol pyrophosphates on cellular energy dynamics. *Science* 334: 802–805.
- Takahashi H, Iwai M, Takahashi Y, Minagawa J. 2006. Identification of the mobile light-harvesting complex II polypeptides for state transitions in *Chlamydomonas reinhardtii*. *Proceedings of the National Academy of Sciences, USA* 103: 477–482.
- Tan X, Calderon-Villalobos LIA, Sharon M, Zheng C, Robinson CV, Estelle M, Zheng N. 2007. Mechanism of auxin perception by the TIR1 ubiquitin ligase. *Nature* 446: 640–645.
- Theis J, Schroda M. 2016. Revisiting the photosystem II repair cycle. *Plant Signaling & Behavior* 11: e1218587.
- Thoreen CC, Chantranupong L, Keys HR, Wang T, Gray NS, Sabatini DM. 2012. A unifying model for mTORC1-mediated regulation of mRNA translation. *Nature* 485: 109–113.
- Thoreen CC, Kang SA, Chang JW, Liu Q, Zhang J, Gao Y, Reichling LJ, Sim T, Sabatini DM, Gray NS. 2009. An ATP-competitive mammalian target of rapamycin inhibitor reveals rapamycin-resistant functions of mTORC1. *Journal of Biological Chemistry* 284: 8023–8032.
- Upadhyaya S, Rao BJ. 2019. Reciprocal regulation of photosynthesis and mitochondrial respiration by TOR kinase in *Chlamydomonas reinhardtii*. *Plant Direct* 3: e00184.
- Vainonen JP, Hansson M, Vener AV. 2005. STN8 protein kinase in *Arabidopsis thaliana* is specific in phosphorylation of photosystem II core proteins. *Journal of Biological Chemistry* 280: 33679–33686.
- Van Leene J, Han C, Gadeyne A, Eeckhout D, Matthijs C, Cannoot B, De Winne N, Persiau G, Van De Slijke E, Van de Cotte B *et al.* 2019. Capturing the phosphorylation and protein interaction landscape of the plant TOR kinase. *Nature Plants* 5: 316–327.
- Vener AV. 2007. Environmentally modulated phosphorylation and dynamics of proteins in photosynthetic membranes. *Biochimica et Biophysica Acta (BBA) – Bioenergetics* 1767: 449–457.
- Vizcaíno JA, Csordas A, del-Toro N, Dienes JA, Griss J, Lavidas I, Mayer G, Perez-Riverol Y, Reisinger F, Ternent T *et al.* 2016. 2016 update of the PRIDE database and its related tools. *Nucleic Acids Research* 44: D447–D456.
- Vizcaíno JA, Deutsch EW, Wang R, Csordas A, Reisinger F, Ríos D, Dienes JA, Sun Z, Farrar T, Bandeira N *et al.* 2014. ProteomeXchange provides globally coordinated proteomics data submission and dissemination. *Nature Biotechnology* 32: 223–226.
- Weiner H, Stitt M, Heldt HW. 1987. Subcellular compartmentation of pyrophosphate and alkaline pyrophosphatase in leaves. *Biochimica et Biophysica Acta (BBA) – Bioenergetics* 893: 13–21.
- Werth EG, McConnell EW, Couso Lianez I, Perrine Z, Crespo JL, Umen JG, Hicks LM. 2019. Investigating the effect of target of rapamycin kinase inhibition on the *Chlamydomonas reinhardtii* phosphoproteome: from known homologs to new targets. *New Phytologist* 221: 247–260.
- Werth EG, McConnell EW, Gilbert TSK, Couso Lianez I, Perez CA, Manley CK, Graves LM, Umen JG, Hicks LM. 2017. Probing the global kinome and phosphoproteome in *Chlamydomonas reinhardtii* via sequential enrichment and quantitative proteomics. *The Plant Journal* 89: 416–426.
- Wild R, Gerasimaite R, Jung J-Y, Truffault V, Pavlovic I, Schmidt A, Saiardi A, Jessen HJ, Poirier Y, Hothorn M *et al.* 2016. Control of eukaryotic phosphate homeostasis by inositol polyphosphate sensor domains. *Science* 352: 986–990.
- Wilson MSC, Livermore TM, Saiardi A. 2013. Inositol pyrophosphates: between signalling and metabolism. *The Biochemical Journal* 452: 369–379.
- Wu M, Chong LS, Perlman DH, Resnick AC, Fiedler D. 2016. Inositol polyphosphates intersect with signaling and metabolic networks via two distinct mechanisms. *Proceedings of the National Academy of Sciences, USA* 113: E6757–E6765.
- Yu L, Chen Y, Tootz SA. 2018. Autophagy pathway: cellular and molecular mechanisms. *Autophagy* 14: 207–215.
- Yu Y, Yoon S-O, Poulgiannis G, Yang Q, Ma XM, Villen J, Kubica N, Hoffman GR, Cantley LC, Gygi SP *et al.* 2011. Phosphoproteomic analysis identifies GRB10 as an mTORC1 substrate that negatively regulates insulin signaling. *Science* 332: 1322–1326.
- Zhu J, Lau K, Puschmann R, Harmel RK, Zhang Y, Pries V, Gaugler P, Broger L, Dutta AK, Jessen HJ *et al.* 2019. Two bifunctional inositol pyrophosphate kinases/phosphatases control plant phosphate homeostasis. *eLife* 8: e43582.

Supporting Information

Additional Supporting Information may be found online in the Supporting Information section at the end of the article.

Fig. S1 Schematic model of InsP₆ phosphorylation steps in *Chlamydomonas reinhardtii*.

Fig. S2 Proteomic workflow for analysis of *Chlamydomonas vip1-1* and wild-type cells treated with rapamycin.

Fig. S3 Global proteomic results.

Fig. S4 Global proteomic gene ontology (GO) analysis for proteins more abundant in *Chlamydomonas vip1-1* and wild-type.

Fig. S5 *Chlamydomonas* wild-type phosphoproteomic gene ontology (GO) analysis.

Fig. S6 Imaging-PAM analysis in *Chlamydomonas* WT and *vip1-1* comparing low (LL) and high light (HL) conditions.

Methods S1 Proteomic analysis additional information and references.

Table S1 Global proteomic analysis of *Chlamydomonas* WT and *vip1-1* strains under control and rapamycin conditions.

Table S2 Phosphoproteomic analysis of *Chlamydomonas* WT and *vip1-1* strains under control and rapamycin conditions.

Table S3 Target of rapamycin (TOR) related targets found in phosphoproteomic analysis of *Chlamydomonas* WT and *vip1-1* strains under control and rapamycin conditions.

Table S4 Photosynthesis-related targets found in global proteomic analysis of *Chlamydomonas* WT and *vip1-1* strains under control and rapamycin conditions.

Table S5 Photosynthesis-related targets found in phosphoproteomic analysis of *Chlamydomonas* WT and *vip1-1* strains under control and rapamycin conditions.

Please note: Wiley Blackwell are not responsible for the content or functionality of any Supporting Information supplied by the authors. Any queries (other than missing material) should be directed to the *New Phytologist* Central Office.